Desalination and Water Treatment
www.deswater.com
doi: 10.5004/dwt.2020.26007

198 (2020) 345–363
September

Comparative study for removal of acid green 20 dye by electrocoagulation technique using aluminum and iron electrodes

Azza M. Shaker[a], Abeer A. Moneer[b,*], Manal M. El-Sadaawy[b], Nabila M. El-Mallah[a], Mohamed SH Ramadan[a]

[a]*Faculty of Science, Chemistry Department, Alexandria University, emails: azzashaker44@gmail.com (A.M. Shaker), dr.nabila.elmallah@gmail.com (N.M. El-Mallah), drmshafek@yahoo.com (M. SH Ramadan)*
[b]*Marine Pollution Department, Environmental Division, National Institute of Oceanography and Fisheries, Alexandria, Egypt, emails: abeermounir30@gmail.com (A.A. Moneer), manal_dn@yahoo.com (M.M. El-Sadaawy)*

Received 17 December 2019; Accepted 17 April 2020

ABSTRACT

Electrocoagulation (EC) process was investigated for the removal of acid green 20 (AG 20) dye from aqueous solutions with a batch-stirred bi-polar system using aluminum (Al) and iron (Fe) electrodes. Many operating parameters were investigated to achieve the best removal conditions to work. The removal percent (% Re) of AG 20 under optimum conditions was 96.38% and 94.81% and the energy consumption was 28.84 and 31.02 (kWh kg^{-1} of the dye) for Fe and Al electrodes respectively. The results showed that increasing the applied current density enhanced the efficiency of removal, which in turn was affected by the type and quantity of added electrolyte. The % Re was adversely affected by pH and initial dye concentration and the optimum values were found to be pH 2 and 60 mg L^{-1} initial dye concentration with both metals. The computed energy consumption and total operating cost confirmed the economic dye removal by the EC technique. 0.5 g NaCl as supporting electrolyte proved to be the ideal quantity and type of supporting electrolyte. The process followed the first-order-rate equation and the thermodynamic studies provided a clear indication that the process is spontaneous and exothermic. Among other models, Freundlich isotherm fitted for Al while Fe followed the postulates of Temkin and Langmuir models. The variation of the electrode set showed that the efficiency of removal with Fe–Fe–Fe–Fe > hybrid > Al–Al–Al–Al. Finally, the correlation matrix and multiple regression analyses were studied and predictive equations were derived.

Keywords: Acid green 20 dye; Adsorption isotherms, Dye removal; Electrocoagulation; Kinetics; Regression analysis

1. Introduction

Water is fundamental to mankind and all living organisms. The pollutants exhibited in water nowadays are entirely unlike those of the past days due to the industrial revolution and related industrial activities, that's why preserving water in our bodies is a very important issue that we have to study very well.

Textile effluents are one of the pollutants that cause environmental contamination. They are severely polluted with the complex organic and inorganic chemicals which are used during various steps of textile processing [1].

The major contaminants in textile effluents are the finishing agents, inhibitors, surfactants, salts, dyes, chlorine compounds, and phosphates, dissolved and suspended solids. The dyes are extremely serious pollutants in the textile effluent; they are used in many industries like leather, paint, rubber, pharmaceuticals, and textiles. They also cause severe damage to humankind like liver dysfunction and

* Corresponding author.

they result in serious damage to the brain, central nervous system, kidneys and the reproductive system [2]. Therefore, the strategy to remove the color or to reduce the dye effect is extremely of significant importance.

Acid dyes have a smaller size and a molecular weight ranging from 200 to 900 [3]. This allows them to migrate from one position to the other very easily and gives a uniform dye application. They are applied to wool, silk, nylon and modified acrylics.

A wide range of technologies is applied for the handling of wastewater like physicochemical processes that include filtration, ion exchange, chemical precipitation, adsorption, chemical oxidation, and ultrafiltration. Also, biological processes and electrochemical techniques are used for wastewater treatment [4], that's why the most effective and cheapest methods for handling wastewater from industrial effluent are inevitable. Electrochemical techniques like electrocoagulation (EC), electro-flotation (EF), electro-decantation and electro-kinetic remediation do not consume a large number of chemicals and they are easily distributed, in addition, their instrumentations are available and achievable.

Generally, coagulation means that the charged particles are neutralized by collision with the counter ions leading to flocculation followed by sedimentation. The EC method replaced the incorporation of metal salts, polymers, and polyelectrolyte for splitting emulsions and suspensions where the dissolution of the anode produces a highly charged metal hydroxide species. These species can remove heavy metals, colloidal particles, and organic and inorganic pollutants from aqueous media [5]. Not only, they can remove textile effluent [1,6–8] but also they can remove oily suspensions [9], heavy metals [10–17], polymeric wastes [18], foodstuff [19] and polishing wastes [20,21], etc.

Because of the existence of dyes of low concentration in water, which causes severe damage in the bodies of water physically and chemically, the handling of dyes from the water poses a great challenge for finding the most effective way of removal. The EC technique has advantages over other techniques such as its simple instrumentation, no addition of chemicals; the water released from this technique is odorless, colorless and clear. It does not produce a high amount of sludge and the sludge that may be formed settable and can be separated easily, the flocs formed can be isolated through sedimentation or flotation and the smallest colloidal particles can also be removed by this method [5].

In the EC process, an electrical current from the direct current source passes between metal electrodes immersed in polluted water. The current passed result in the dissolution of the metal used into the water in the form of ions. At a suitable pH, the ions produced can form a broad range of polymeric species (i.e. metal hydroxides). These species cause destabilization and aggregation of the suspended particles or precipitation of the adsorbed contaminants.

EC has been reported to be efficient in removing dyes from water. The metals mostly used in the EC process as electrodes are aluminum and iron because of the formed amorphous $Al(OH)_{3(s)}$ and $Fe(OH)_3$ flocs have a great surface area. The importance of these flocs is derived from their ability to remove the organic compounds through adsorption and trapping of colloidal particles. These flocs can be removed by either sedimentation or H_2 flotation.

In the present work, the achievement of the EC system in the removal of acid green 20 (AG 20) from synthetic wastewater has been investigated to find out which electrode metal Al or Fe is more efficient for removing the dye. Also, the study aims to explore the effect of varying the operating parameters such as the applied current density (CD), initial dye concentration, pH of the solution, and the effect of electrolyte attempting to optimize each parameter. The mechanism, kinetics, and thermodynamic studies were investigated.

2. Experimental setup

2.1. Materials

The experiments were conducted using AG 20 dye solutions. The structure of the dye and the main characteristics are illustrated in Fig. 1 and Table 1 respectively.

The solution was prepared by dissolving the desired weight of the dye into distilled water and diluted to the desired concentration. The pH was adjusted with (0.5 M) HCl and (0.5 M) NaOH. Sodium chloride, sodium sulfate, sodium acetate, sodium carbonate, and sodium bicarbonate were utilized as supporting electrolytes. All chemicals were obtained from the Chemajet chemical company Egypt with 99% purity. Iron (Fe) and/or aluminum (Al)

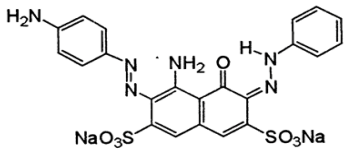

Fig. 1. Chemical structure of acid green 20.

Table 1
Characteristics of acid green 20

International Union of Pure and Applied Chemistry (IUPAC) name	Disodium 4-amino-3-[(4-aminophenyl)azo]-5-hydroxy-6-(phenylazo)naphthalene-2,7-disulphonate
CAS number	5850-39-5
Molecular formula	$C_{22}H_{16}N_6Na_2O_7S_2$
Molecular weight	586.51 g mol^{-1}
Color index number	20,495
UV absorption	λ_{max} 634 nm

plates (purity: 80% and 100% respectively, a product of Egyptian Copper Company, Alexandria, Egypt).

2.2. Experimental apparatus

A laboratory bench-scale EC unit was designed and constructed with the dimensions represented in Fig. 2a. Nine sheets of aluminum and iron electrodes were used with a surface area equal to 124.8 cm^2. Their number and type varied according to the experiment. The electrodes were, dipped in HCl solution, polished with emery paper and cleaned with distilled water to remove impurities and metal hydroxide precipitates from the electrode surface. The cell is represented in Fig. 2a [14] where the electrodes are attached to DC power supply in a bi-polar arrangement in series connection as illustrated in Fig. 2b [22].

2.3. Analytical methods

The dye concentrations were determined by the JASCO V-350 UV-Vis spectrophotometer, Japan. The Beer–Lambert law ($A = \varepsilon \times \ell \times C$) was applied at the desired wavelength (λ = 634 nm), where ε was the molar absorptivity, ℓ was the cell thickness and C was the dye concentration.

Various standard concentrations of dye were analyzed by spectrophotometer measurement to draw the calibration curve. The data of different conditions were obtained and the percentage removal of the AG 20 (% Re) was computed using the following equation:

$$\%\ \mathrm{Re} = \left(\frac{C_0 - C_t}{C_0}\right) \times 100 \tag{1}$$

where C_0 and C_t are the initial and concentrations of dye at a time (t), respectively.

The pH of the solution was adjusted and measured by pH meter (HANNA instruments HI 8014, USA). The stirring rate and the temperature were adjusted using a magnetic stirrer hot plate (FALC instruments F60 stirrer with heating).

The quantity of adsorbed dye at equilibrium q_e mg g^{-1} was calculated using Eq. (2):

$$q_e = \frac{\left(C_0 - C_e\right)V}{W} \tag{2}$$

where C_0 and C_e are the initial and equilibrium concentration of AG 20 in mg L^{-1}. V is the solution volume in L and W is the mass of the metal coagulant used in grams and it can be calculated from the following Eq. (3):

$$W = \frac{MIt}{nF} \tag{3}$$

where M stands for the molar mass in g mol^{-1} of the elements, I represents the current in A, t is the electrolysis time in seconds, n represent the number of electrons involved in the reaction and F stands for Faraday's constant (96,485 C per mol of electrons).

3. Results and discussion

3.1. Effect of pH

To assess the effectiveness of pH on the % Re of AG 20, a series of experiments were performed by varying the initial pH from 2.0 to 11.0. Fig. 3 shows the influence of pH on the removal of the dye. It can be observed that the favorable pH value, which gives the highest removal capability, is 2.0 for both metals Al and Fe.

The reactions taking place with metal M (either Al or Fe) as an anode may be summarized as follows:

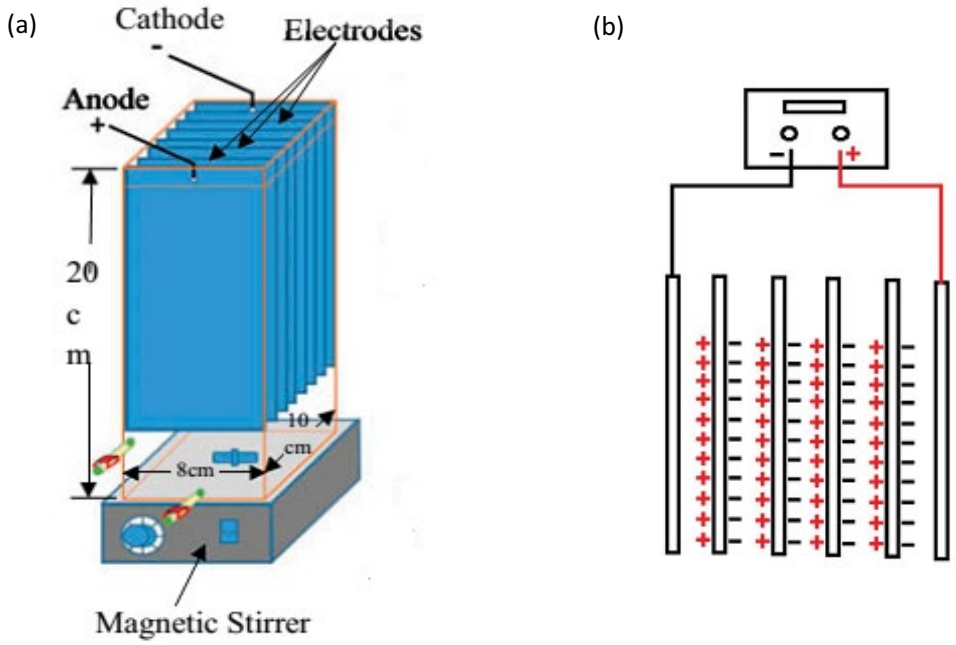

Fig. 2. (a) Schematic diagram of setup and (b) bipolar electrodes in series connection.

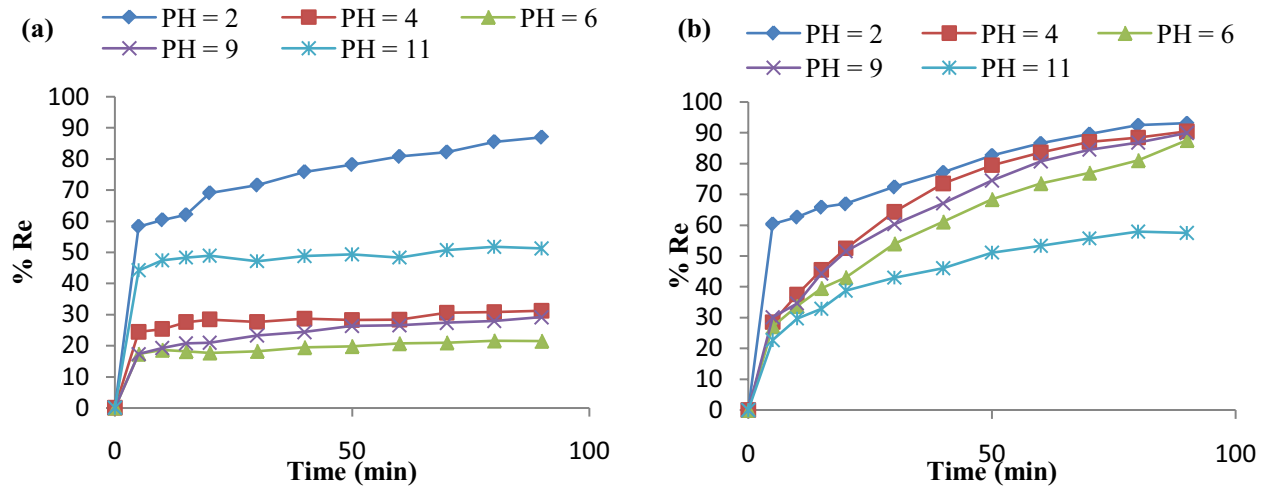

Fig. 3. Effect of initial pH on the removal of dye at different time intervals (CD = 40 mA cm^{-2}; C_0 = 60 mg L^{-1}; t_{EC} = 90 min; stirring speed = 771.4 rpm; nine electrode sheets; RT) (a) Al electrodes and (b) Fe electrodes.

- At the anode:

$$M_s \rightarrow M_{aq}^{n+} + ne^- \quad (4)$$

$$2H_2O \rightarrow 4H_{aq}^+ + O_{2(g)} + 4e^- \quad (5)$$

- At the cathode:

$$M_{aq}^{n+} + ne^- \rightarrow M_s \quad (6)$$

$$2H_2O + 2e^- \rightarrow H_{2(g)} + 2OH^- \quad (7)$$

According to the pH of the medium, in aqueous medium aluminum ions can give a complex equilibrium with different monomeric species like $Al(OH)^{2+}$, $Al(OH)_2^+$, $Al(OH)_3$ and $Al(OH)_4^-$. These species can be polymerized into $Al_2(OH)_2^{4+}$, $Al_6(OH)_{15}^{3+}$, $Al_7(OH)_{17}^{4+}$, $Al_8(OH)_{20}^{4+}$, $Al_{13}O_4(OH)_{24}^{7+}$ and $Al_{13}(OH)_{34}^{5+}$ [22].

In case of Fe, Barrera-Díaz et al. [23] reported that $Fe(OH)_3$ is in equilibrium with many soluble monomeric species as a function of pH range as the following: Up to pH 2.0: $Fe(OH)_3$ is in equilibrium with Fe^{+3} and at pH 2.0 to 3.8 $Fe(OH)_3$ is in equilibrium with $Fe(OH)^{2+}$. At pH 3.8 to 6.2; $Fe(OH)_3$ is in equilibrium with $Fe(OH)_2^+$ and at pH 9.6 $Fe(OH)_3$ is in equilibrium with $Fe(OH)_4^-$. Also, complexes like $Fe(OH)_2^{4+}$ and $Fe_2(OH)_4^{2+}$ can exist in the pH range of 3.5–7.0.

Table 2 indicates the influence of initial pH on the % Re of AG 20 dye and how the pH of the medium changes during the process of EC. As can be noticed from results; in the case of using Al electrodes, the final pH did not reveal a great change from the initial value in the acidic medium while in the case of Fe the final pH increased. From the equations (4–7) the reactions produce OH^- in the solution greatly affects the pH of the medium (i.e. pH should increase in acidic medium). In the case of aluminum, the alkalinity produced was insufficient to increase the pH of the medium [24]. Regarding the pH drop which takes place when the initial pH is above 9, this may be owing to the dissolution reaction of the metal hydroxide to either $[Al(OH)_4]^-$, $[Fe(OH)_3]^-$ and $[Fe(OH)_4]^-$ where the formed species consumes the OH^- from the medium (i.e. alkalinity consumers).

By inspecting Fig. 3, it can be deduced that in the first few minutes the % Re reached 60% with both metals at pH 2 and it started to increase with time in both cases. In the case of using Fe electrodes and with all tried pHs the % Re started with sudden increase and continued to increase through the experiment time. On the other hand, in case of using Al electrodes, the % Re that was achieved in the first few minutes kept constant all over the experiment time, which means that the alteration of pH took place at this

Table 2
Effect of initial pH of dye solution on the removal efficiency of AG 20 dye

Al			Fe		
pH_i	pH_f	% Re	pH_i	pH_f	% Re
2.04	2.03	87.02%	2.06	5.52	93.06%
4.10	4.26	31.42%	4.11	6.30	90.45%
6.15	6.28	21.50%	6.00	6.33	87.59%
9.12	8.09	29.16%	9.10	8.85	89.90%
11.03	9.30	51.31%	11.01	10.75	57.43%

time and remains constant to the end of the experiment and consequently no alteration in the % Re took place along the experiment. This was not the case with pH 2, and this signifies that severe acidic medium is the appropriate medium for the removal of this dye whatever the electrode's metal is.

3.2. Effect of initial dye concentration (C_0)

Fig. 4 shows effect of initial dye concentration on the removal efficiency at different time intervals. The impact of C_0 on % Re of the dye was studied by varying AG 20 concentration from 50 to 150 mg/L. The % Re was 86%, 87%, 82.62%, 82.5%, and 78.25% for dye concentrations of 50, 60, 80, 100 and 150 ppm respectively using Al as electrodes and 87.4%, 87%, 86.4%, 83.45%, and 75.2% with the same set of concentrations with Fe metal as electrodes and the optimum concentration was detected at 60 mg L^{-1} when using either metal.

The results showed that the % Re of AG 20 is reduced with increasing the initial dye concentration. As stated by Faraday's law, the quantity of metal ions [Al^{+3}, Fe^{+3}] passing to the solution at the same current density and time for all dye concentrations is constant and consequently, the number of flocs generated in the solutions would be the same. Consequently, the flocs that are generated at high dye concentration were inadequate to adsorb all the AG 20 molecules in the solution. This means that increasing the dye concentration will cause a reduction in the rate of dye removal considerably [25–27].

3.3. Effect of supporting electrolyte

Supporting electrolytes are used to reduce the Ohmic drop, the energy consumption and increase the solution conductivity. Also, the electrolyte can influence the dissolution kinetics of the anode. It also has a major impact on the double layer shielding by the coagulation process [28–31].

Fig. 5 illustrates the influence of 0.5 g L^{-1} of different supporting electrolytes on the % Re of AG 20. It can be

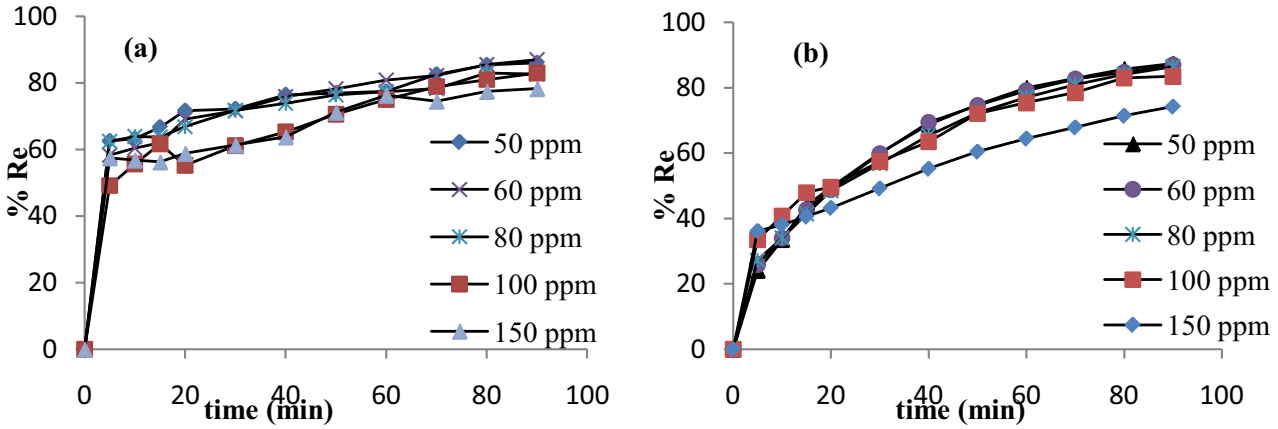

Fig. 4. Effect of initial dye concentration on the removal efficiency at different time intervals (CD = 40 mA cm^{-2}; time of EC (t_{EC}) = 90 min; stirring speed = 771.4 rpm; nine electrode sheets; room temperature (RT), (a) Al electrodes where pH_i = 2 and (b) Fe electrodes where pH_i = 5.8).

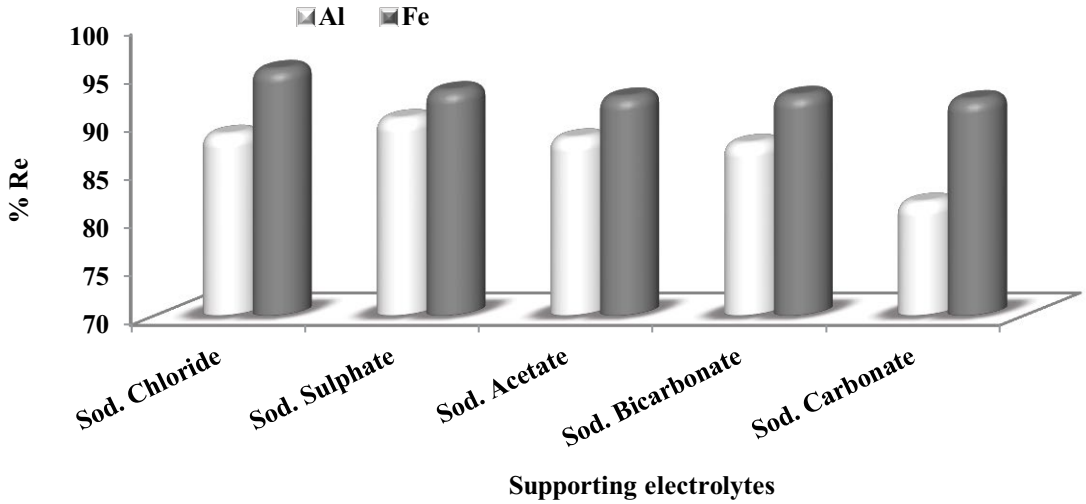

Fig. 5. Effect of 0.5 g L^{-1} for different supporting electrolytes on the removal efficiency of the dye (CD = 40 mA cm^{-2}; C_0 = 60 mg L^{-1}; pH_i = 2; t_{EC} = 90 min; stirring speed = 771.4 rpm; nine electrode sheets; RT).

observed that in the case of Al electrodes the removal has reached 90% in the case of Na_2SO_4 while it reached 88% in the case of NaCl, CH_3COONa, and $NaHCO_3$ while it was 81.6% in the case of Na_2CO_3 after 90 min of EC. However, the higher removal observed after a long time of EC can be ascribed to the higher positive potential applied.

The variation between the electrolytes used can be detected in the operating time at the first 20 min of EC using Al electrodes where the NaCl led to the higher percent removal corresponding to the following results 77%, 72.2%, 65%, 64% and 61% removal for NaCl, CH_3COONa, Na_2SO_4, $NaHCO_3$, and Na_2CO_3 respectively as represented in Fig. 6.

Also in the case of Fe electrodes (Fig. 5), the higher removal efficiency gave 95.35% using NaCl electrolyte while % Re 93.16%, 92.5%, 92.67%, and 92.23% were obtained with Na_2SO_4, CH_3COONa, $NaHCO_3$, and Na_2CO_3 respectively.

Due to the corrosive power of the chloride ions where it causes localized pitting corrosion with the aluminum surfaces, it has a higher removal efficiency than the other ions and due to this ability to release the coagulant species, it requires much lower voltage for the dissolution process. Alternatively, the sulfate ions can form complexes with the Al and cause passivation to the anodic surface. So they need more positive potential to overcome the passivation [32].

The chloride ions also can undergo oxidation reactions as given by Eqs. (8)–(10):

$$2Cl^- \rightarrow Cl_{2(aq.)} + 2e^- \quad (8)$$

$$Cl_{2(aq.)} + H_2O \rightarrow HClO + Cl^- + H^+ \quad (9)$$

$$HClO \leftrightarrow ClO^- + H^+ \quad (10)$$

These high oxidant chlorine species are responsible for the characteristic pitting corrosion (i.e. more oxidation to the anodic surfaces) in addition to they help in oxidation of organic matter.

Owing to the large size of the acetate ion it requires a much longer time to travel to electrode surfaces and to have an influence on the cathodic reactions and also as a result of the competitive adsorption effect between the dye and the acetate ion [33]. Furthermore, the carbonate and bicarbonate ions have minimum removal efficiency. This may be attributed to the passivation of the electrode surfaces. The passivation increases the overall resistance leading to a rise in the cell potential without affecting the coagulant or the bubble production rates [34].

Fig. 7 represents the influence of NaCl concentration on the removal of AG 20. In the Al electrode, it was found that increasing the NaCl concentration result in a reduction in the % Re this may be a result of the rise in the competition between the ions and the retardation force of the inter-ionic attraction [33]. The lower concentration of supporting electrolyte was found to give higher removal efficiency. Taking these results into consideration, the lower concentration (0.5 g L^{-1}) was chosen to be the optimum concentration to use.

In Fe electrodes, increasing the concentration of NaCl almost does not affect, so the best concentration should be used was found to be 0.5 g L^{-1} to avoid the competition between the ions.

In comparison between Al and Fe Fig. 7 demonstrates the removal efficiencies of 88.64% and 95.35% for Al and Fe respectively. Consequently, Fe was selected as a better metal than Al in the EC process for the removal of AG 20 dye.

3.4. Effect of current density

To study the influence of the current density on the removal of AG 20, the EC procedure was performed by trying the following current densities: 8.01, 40.06, 64.10 and 100.16 mA cm^{-2}. Fig. 8 indicates that the % Re increases up to 88.64% by raising the current density to 40.06 mA cm^{-2} in the case of Al electrodes, and it started to decline with the upper current densities to reach 81.77% with current density 100.16 mA cm^{-2}. This may result from the destruction of the flocs by the excessive formation of H_2 gas on the cathode side [35]. Alternatively, the removal improved up to 95.97%

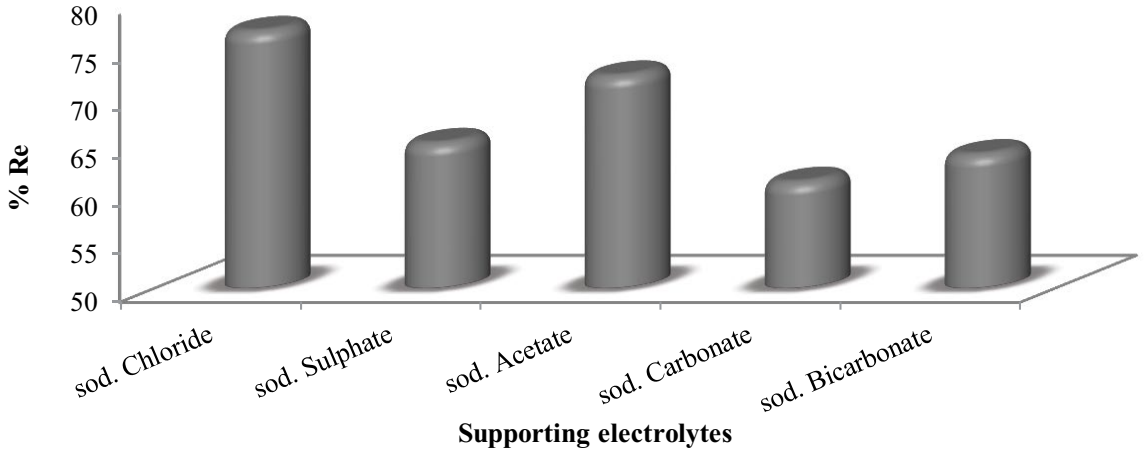

Fig. 6. Effect of 0.5 g L^{-1} for different supporting electrolytes on the removal efficiency for Al metal (CD = 40 mA cm^{-2}; C_0 = 60 mg L^{-1}; pH_i = 2; t_{EC} = 20 min; stirring speed = 771.4 rpm; nine electrode sheets; RT).

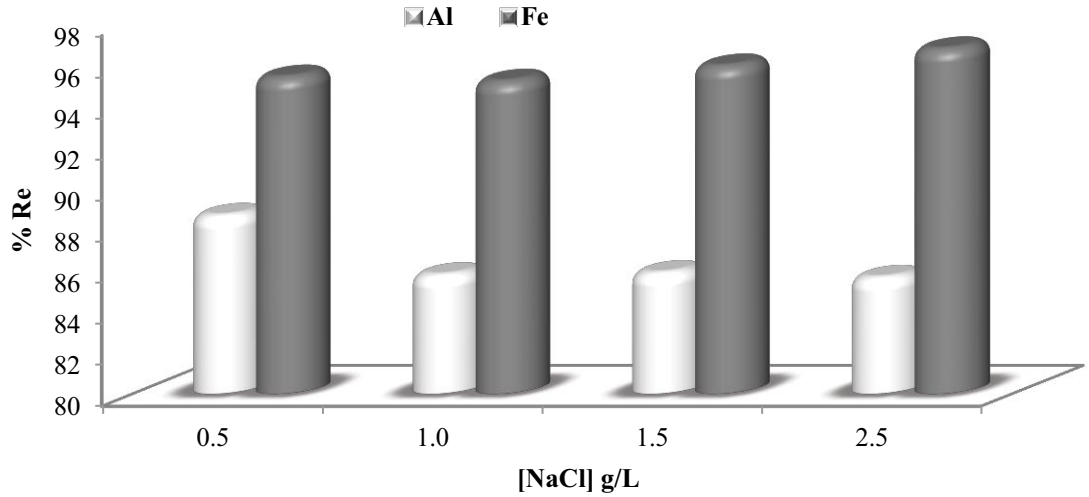

Fig. 7. Effect of the concentration of NaCl on the removal efficiency (CD = 40 mA cm^{-2}; C_0 = 60 mg L^{-1}; pH$_i$ = 2; t_{EC} = 90 min; stirring speed = 771.4 rpm; nine electrode sheets; RT).

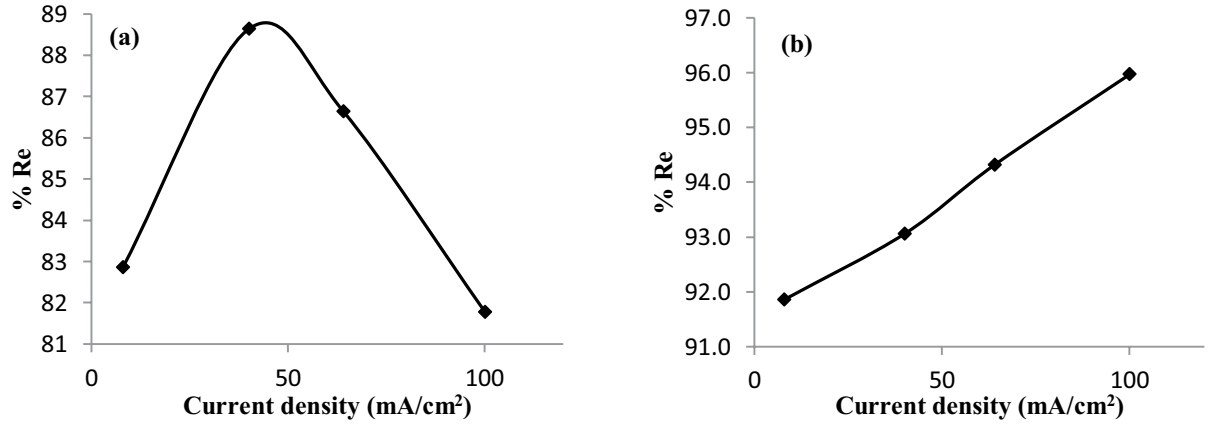

Fig. 8. Effect of current density on removal efficiency of AG 20 (NaCl = 0.5 g L^{-1}; C_0 = 60 mg L^{-1}; pH$_i$ = 2; t_{EC} = 90 min; stirring speed = 771.4 rpm; nine electrode sheets; RT) (a) Al metal and (b) Fe metal.

with raising the current density to 100.16 mA cm^{-2} in the case of Fe electrodes. The improvement in the % Re may be due to the growth in the ions that are produced on the electrodes, resulting in aggregation and increasing the hydrogen evolution where it is familiar that the current density regulates the assembly of the coagulant, bubbles and the development of flocs.

3.5. Energy consumption

To assess the viability of the EC process not only the removal efficiencies are of great importance, but the energy consumption calculations to further support the economic feasibility of the EC process are important as well.

The energy consumption in kWh kg^{-1} of the dye can be estimated from Eq. (11) [36,37]:

$$\text{Energy consumption}\left(\text{kWh/kg of dye}\right)=\frac{V\times I\times t}{\left(C_0-C_t\right)\times v} \quad (11)$$

where V stands for the applied voltage (volt), I denotes the applied current (A), t signifies the time (hour), C_0 denotes the initial concentration of the dye, C_t stands for the concentration at time t and v is the working volume (L). It is noteworthy that under the optimum conditions of C_0 = 60 mg L^{-1} of both dyes, 0.5 g L^{-1} NaCl supporting electrolyte, pH$_i$ = 2, 90 min of operation, stirring speed = 771.4 rpm, nine electrode sheets and at room temperature, the energy consumption was 28.84 and 31.02 (kWh kg^{-1} of the dye) for Fe and Al electrodes respectively using a current density of 40 mA cm^{-2}.

The influence of NaCl concentration on energy consumption is represented in Fig. 9. It can be noticed that Fe consumes much less energy than Al and consequently, Fe was found to be a better metal than Al in the EC process for the removal of AG 20 dye.

In addition, Fig. 10 illustrates the effect of current density on energy consumption. It is clear that the current density raises the energy consumption so it is not preferred to use a very high current density since it consumes more

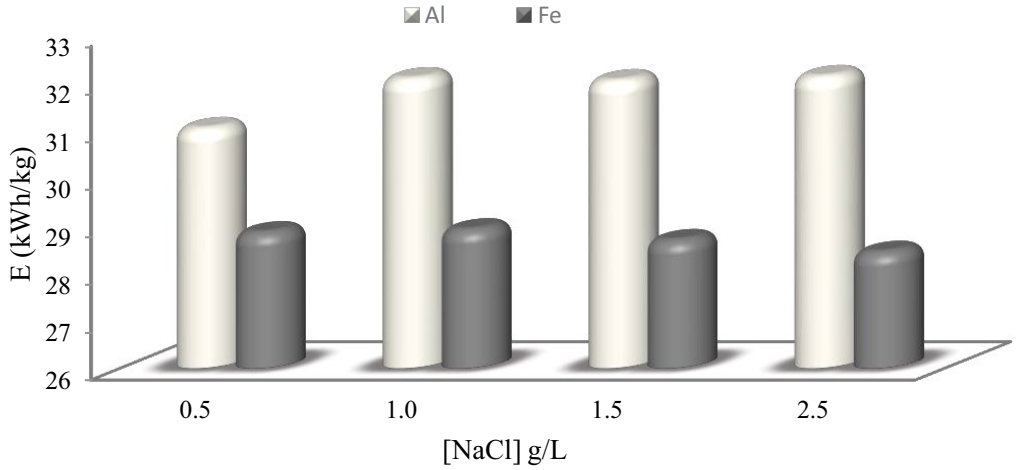

Fig. 9. Effect of the concentration of NaCl (g L^{-1}) on the energy consumption (CD = 40 mA cm^{-2}; C_0 = 60 mg L^{-1}; pH_i = 2; t_{EC} = 90 min; stirring speed = 771.4 rpm; nine electrode sheets; RT).

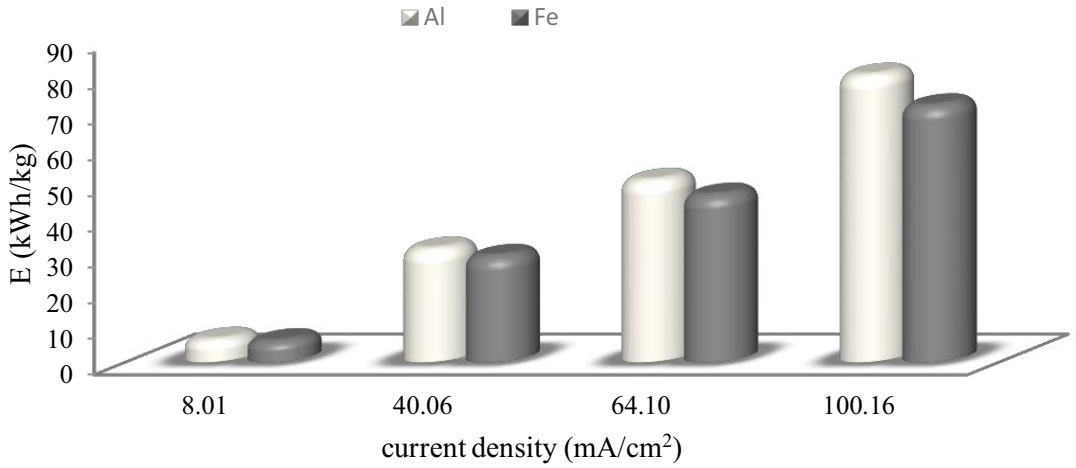

Fig. 10. Effect of current density on energy consumption (NaCl = 0.5 g L^{-1}; C_0 = 60 mg L^{-1}; pH_i = 2; t_{EC} = 90 min; stirring speed = 771.4 rpm; nine electrode sheets; RT).

energy and gives lower removal efficiency in some cases, or the best cases; the same removal efficiency. Also as illustrated Fe electrodes utilize less energy than the Al electrodes which indicates that the Fe is much better than the Al electrodes. It can also be seen that using Al electrodes consumes much energy with greater current densities than the lower ones with no increase in percent removal but on contrary with a decrease in it. Furthermore, the energy consumption of Fe electrodes is much less than Al electrodes when using higher current densities, this remark was not seen with lower current densities, where it can be found that there is almost no alteration among the energy consumptions with the two metals. Consequently, and for all these reasons it is recommended to use Fe electrodes for the removal of AG 20 under optimum conditions achieved.

3.6. Effect of stirring rate

Stirring the solution helps to maintain the uniform conditions and avoids the emergence of a concentration gradient in the electrolysis cell. Furthermore, the agitation in the electrolysis cell will increase the velocity of the produced ions.

Fig. 11 illustrates the influence of the stirring rate (257.14, 771.42, 1,285.7 and 1,800 rpm) on the % Re of the dye. The calculated values of the % Re were 85.0%, 88.6%, 84.0% and 84.3% respectively for Al while the values were 94.3%, 95.3%, 95.5% and 95.9% respectively for Fe. The optimum value was found to be at the medium speed of agitation which is 771.42 rpm for both metals. This may be attributed to the insufficient mixing of the coagulant with the dye at a lower speed while increasing the speed of agitation up to the optimum stirring rate 771.42 rpm, there is an increase in the % Re of the dye. Owing to the increase in the mobility of the produced ions, the flocs are generated much faster leading to an increase in the % Re of the dye for a particular electrolysis time [38]. Regarding the aluminum; an additional rise in the agitation speed beyond the optimum value a reduction in % Re of the dye is obtained where the flocs got degraded by collision with

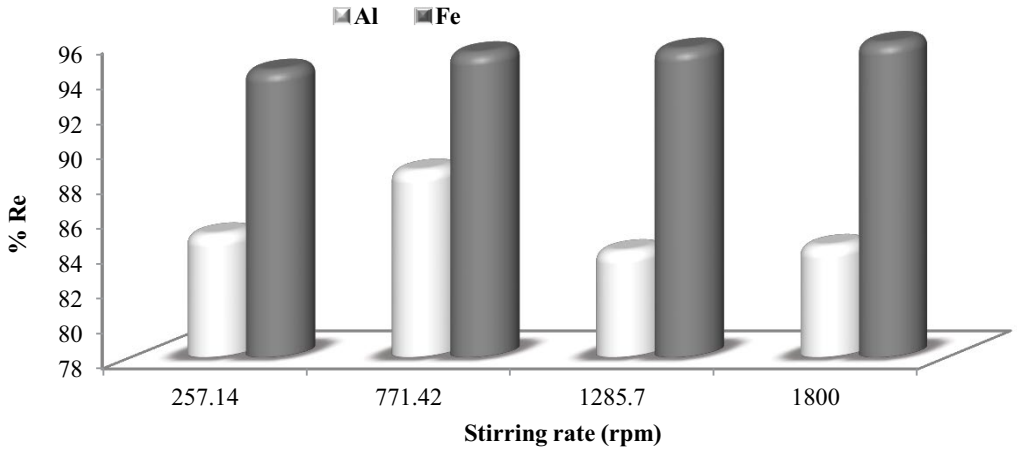

Fig. 11. Effect of stirring rate on the removal efficiency of AG 20 dye (CD = 40 mA cm^{-2}; C_0 = 60 mg L^{-1}; NaCl = 0.5 g L^{-1}; pH_i = 2; t_{EC} = 90 min; nine electrode sheets; RT).

each other due to high agitation speed [7]. In the case of Fe, the removal is almost the same from 771.42 to 1,800 rpm, indicating that the flocs are stable at the higher speed of agitation and do not degrade.

3.7. Effect of the number of electrodes

Fig. 12 demonstrates the relationship between the percent removals of the AG 20 dye with the number of electrodes (2–9 electrodes). The presented results point out that increasing the electrode number leads to an increase in % Re to 88.64% with 9 electrodes in the case of Al and to 95.35% in the case of Fe.

The surface area that generates the coagulants in the EC process increase with increasing the number of electrodes and consequently the Al and Fe polymers increase, leading to an increase in the % Re [38].

It can be noticed that enlarging the number of electrodes from 2 to 9 in case of using Al electrodes increases the % Re by almost 25%, while in case of using Fe electrodes the increase was about 33%, which stresses the fact that the rate of metal dissolution of iron is greater than that of aluminum. Remarkably, it can be seen that the insignificant change in % Re with Fe electrodes from 6 to 9 electrodes, is a very important point for saving the cost of treatment; from an economic point of view. Accordingly, it must be followed to estimate the most appropriate number of electrodes to get the maximum % Re.

3.8. Effect of distance between two electrodes

Fig. 13 represents the relation between the % Re of AG 20 dye and the gap between two electrodes. The optimum distance was noticed to be 5 cm & 3.5 cm for Al and Fe respectively. It is observed that a very short gap between the electrodes results in lower removal efficiency (60.14% with Al and 68.77% with Fe). This may be due to increasing the electrostatic impact that prevents the collision of the particles. Also, with enlarging the gap between the two electrodes the removal started to increase up to 69% with Al and 77.7% with Fe owing to the decrease in electrostatic effects which result in a slower movement in the formed ions providing enough time for the produced metal hydroxides to aggregate and produce the flocs. This results in increasing the % Re of AG 20 dye in the solution [1,34].

Further enlargement in the distance results in a reduction in the production of the flocs and consequently, the removal will decrease (59.93% and 71.3% for Al and Fe respectively). This may be ascribed to the increase in the travel time of the ions with enlargement of the gap between the electrodes and the decrease in electrostatic attraction resulting in less formation of the flocs needed for coagulation [22,34].

3.9. Effect of temperature

Like any other chemical reaction rates, the electrochemical reaction rates increase with raising the solution temperature. Fig. 14 represents the increase in the % Re with increasing the temperature where the % Re has reached 94.81% and 96.38% at 318 and 308 K for Al and Fe respectively. This may be attributed to the rise in thermal agitation which is responsible for increasing the mobility and collision of the ions with the hydroxide polymers. An additional rise in temperature did not give a great alteration in the removal efficiency.

The thermodynamic parameters (standard Gibbs free energy change ($\Delta G°$), standard enthalpy change ($\Delta H°$) as well as standard entropy change ($\Delta S°$) were estimated by Eqs. (12) and (13):

$$\Delta G° = -RT \ln K_d \tag{12}$$

$$\ln K_d = \frac{\Delta S°}{R} - \frac{\Delta H°}{RT} \tag{13}$$

The equilibrium constant K_d was obtained from q_e/C_e at equilibrium condition in various temperatures where q_e stands for the quantity of the adsorbed dye (mg g^{-1}), C_e denotes the equilibrium concentration of adsorbate, R is the ideal gas constant (8.314 J mol^{-1} K^{-1}) and T (K) stands for the absolute temperature. The plot of $\ln K_d$ vs. $1/T$ provides a straight line of intercept equal $\Delta S°/R$ and a slope equivalent

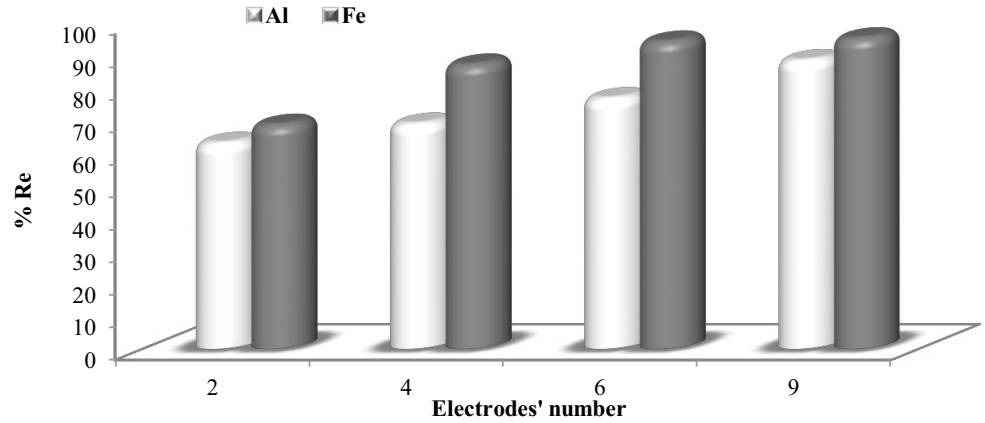

Fig. 12. Effect of the number of electrodes on the removal efficiency (CD = 40 mA cm^{-2}; C_0 = 60 mg L^{-1}; NaCl = 0.5 g L^{-1}; pH_i = 2; t_{EC} = 90 min; stirring speed = 771.4 rpm; RT).

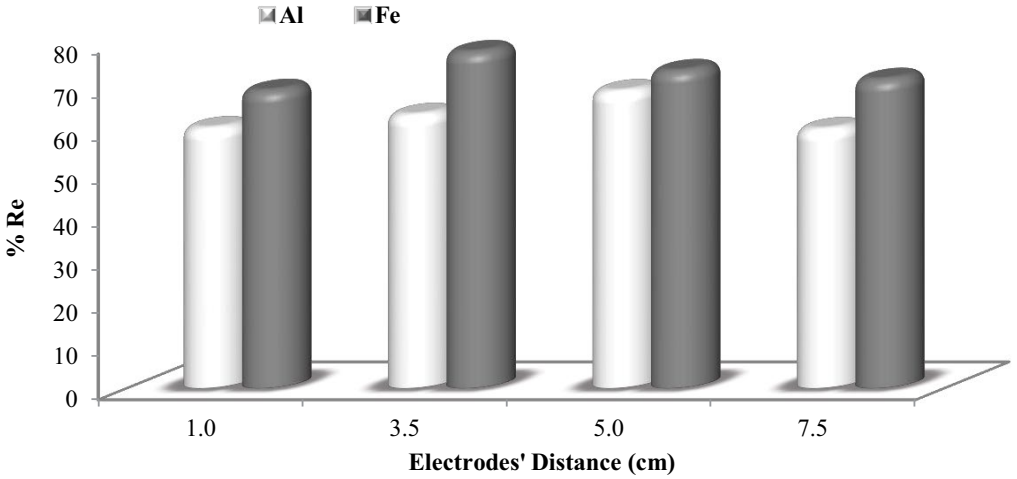

Fig. 13. Effect of distance between two electrodes (CD = 40 mA cm^{-2}; C_0 = 60 mg L^{-1}; NaCl = 0.5 g L^{-1}; pH_i = 2; t_{EC} = 90 min; stirring speed = 771.4 rpm; RT).

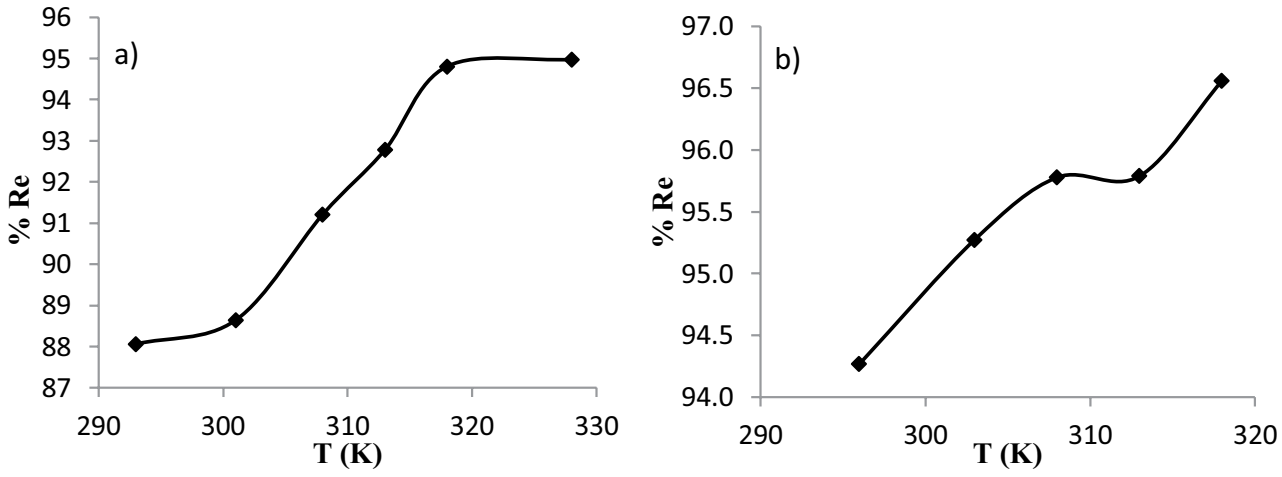

Fig. 14. Effect of temperature on the removal efficiency of AG 20 (CD = 40 mA cm^{-2}; NaCl = 0.5 g L^{-1}; C_0 = 60 mg L^{-1}; pH_i = 2; t_{EC} = 90 min; stirring speed = 771.4 rpm; nine electrode sheets) (a) Al metal and (b) Fe metal.

to $-\Delta H°/R$ [31]. The calculated thermodynamic parameters obtained from the EC process are illustrated in Table 3.

The negative $\Delta G°$ values verified the spontaneity of the removal of AG 20 through the adsorption mechanism. The positive value of $\Delta S°$ reflected the randomness of the process and the negative value $\Delta H°$ pointed out that the process is exothermic. Comparing Al with Fe, the iron metal is preferred than the aluminum since $\Delta G°$ value was found to be more negative at the optimum temperature indicating a favorable spontaneous adsorption process while $\Delta S°$ value was found to be less positive for Fe rather than Al which highlighted that the process of adsorption is more ordered for Fe rather than Al.

4. UV-Vis absorption spectra of acid green 20

The spectral change of AG 20 dye with Al and Fe electrodes can be illustrated in Fig. 15. It can be realized that the removal process is faster and higher in the case of Fe where the removal has reached 94.7% after 60 min EC while in Al it reached 84.03% after 90 min EC under identical conditions of electrolysis. Also, the spectra pointed out that the absorbance of AG 20 at λ_{max} decreased with time and no new band appeared. It means that there were no intermediates formed within the process and the dye did not degrade or break down.

5. Applied adsorption isotherms

The mechanism of adsorption was studied using four adsorption isotherms models namely Langmuir, Freundlich, Dubinin–Radushkevich and Temkin. Various constants, as well as correlation coefficients for adsorption of AG 20 onto the flocs, were determined to identify the best fit model for the adsorption process. The linear form of the studied models is tabulated in Table 4.

5.1. Langmuir isotherm

Assuming that the entire surface for the adsorption method has the same activity, no interaction among adsorbed species and all the adsorption processes have an identical mechanism. The linear Langmuir isotherm model which was derived by Irving Langmuir [39] is presented in Table 4.

A graph of $1/q_e$ vs. $1/C_e$ was plotted to obtain q_m and K_a which are obtained from the intercept and slope of the line. Also, the values of correlation coefficient (R^2) are given in Table 5

It is noticed that R^2 value in the case of Al is close to unity and equal to 0.9855 as shown in Table 5, whilst a negative value of Langmuir isotherm constants is obtained. This refers to the inadequacy of this model for the representation of adsorption technique as those constants are representative of monolayer coverage and surface binding energy [40,41]. This indicates the insufficiency of this model for representing the adsorption technique and contradicts the found results of some adsorption studies by other researchers [42].

Dimensionless constant R_L represents the intensity of adsorption:

$$R_L = \frac{1}{\left(1 + K_a C_0\right)} \tag{14}$$

If $R_L = 0$ then it is irreversible, favorable if $0 < R_L < 1$, linear if $R_L = 1$ and unfavorable if $R_L > 1$. The value of R_L as demonstrated in Table 5 is 0.268 indicating a favorable adsorption process in case of Fe metal.

5.2. Freundlich isotherm

It describes the non-ideal and reversible adsorption process. This model can be illustrated in Table 4 [43].

It has been reported if n_f equal 1 then the division among the two phases does not depend on the concentration and if the value of $1/n_f$ is lower than one it shows normal adsorption while it is cooperative adsorption if $1/n_f$ is above one [44].

The calculated parameters are demonstrated in Table 5 where the values of R^2 are 0.991 and 0.855 for Al and Fe, respectively. In the case of Al, a good straight line was obtained and it is mostly fitted to this model contrary to the Fe Freundlich isotherm model which is unfavorable.

5.3. Dubinin–Radushkevich isotherm [45]

This type of isotherm can determine the kind of adsorption mechanism whether it is physical or chemical adsorption [45]. It is mainly applied to the heterogeneous surfaces with porous structure. The Dubinin–Radushkevich isotherm equation as illustrated in Table 4.

Table 3
Thermodynamic parameters for the removal of AG 20 by EC technique

Aluminum				Iron			
T (K)	$\Delta G°$ (kJ mol^{-1})	$\Delta S°$ (J mol^{-1} K^{-1})	$\Delta H°$ (kJ mol^{-1})	T (K)	$\Delta G°$ (kJ mol^{-1})	$\Delta S°$ (J mol^{-1} K^{-1})	$\Delta H°$ (kJ mol^{-1})
293	–2.620	90.473	–24.053	**296**	–3.374	62.653	–15.215
303	–2.832			**303**	–3.686		
308	–4.133			**308**	–4.177		
313	–3.731			**313**	–4.259		
318	–5.241			**318**	–4.793		
328	–5.501						

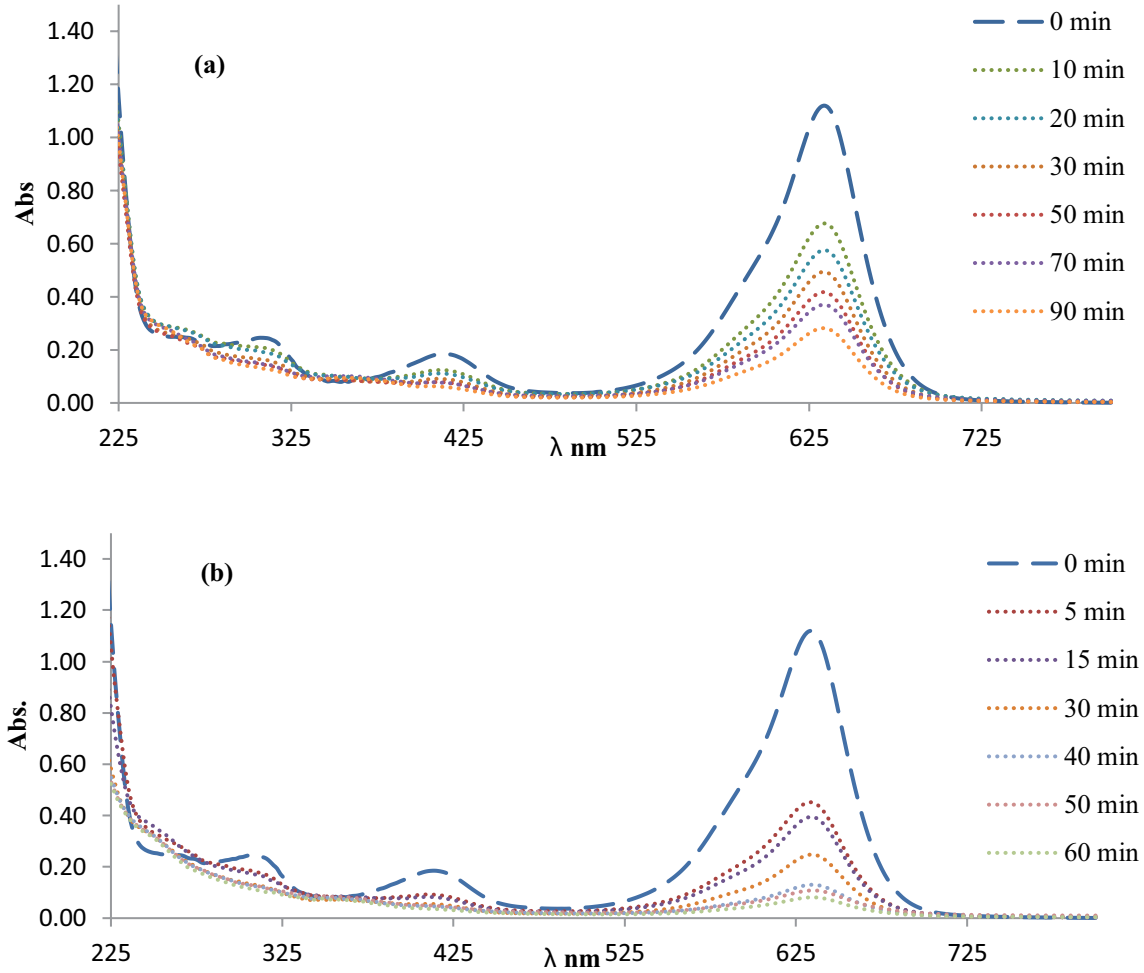

Fig. 15. The spectral changes of the AG 20 dye with (a) Al electrodes and (b) Fe electrodes (CD = 40 mA cm^{-2}; NaCl = 0.5 g L^{-1}; C_0 = 60 mg L^{-1}; pH$_i$ = 2; stirring speed = 771.4 rpm; nine electrode sheets).

Table 4
The linear form of the applied isotherm models

Isotherm name	Linear form	Parameters
Langmuir	$\frac{1}{q_e}=\left[\frac{1}{K_a q_m}\right]\frac{1}{C_e}+\frac{1}{q_m}$	q_m (mg g^{-1}) K_a (L mg^{-1})
Freundlich	$\ln q_e = \ln K_f + \frac{1}{n_f}\ln C_e$	K_f ((mg g^{-1})(L mg^{-1}), $1/n_f$)
Dubinin–Radushkevich	$\ln q_e = \ln q_m - K_{DR}\varepsilon^2$ $\varepsilon = RT\ln\left(1+\frac{1}{C_e}\right)$	K_{DR} (mol^2 kJ^{-2})
Temkin	$q_e = B_T \ln A_T + B_T \ln C_e$ $B_T = (RT)/b_T$	A_T (L g^{-1}) b_T

Table 5
Different parameters of adsorption isotherm models

Isotherm model	Parameters	Values	
		Aluminum	Iron
Langmuir	K_a (L mg^{-1})	–0.034	0.045
	q_m (mg g^{-1})	–68.03	200.0
	R_L	–0.953	0.268
	R^2	0.985	**0.940**
Freundlich	K_f (mg g^{-1})	1.067	9.374
	n_f	0.655	1.205
	R^2	**0.991**	0.855
Dubinin–Radushkevich	q_m (mg g^{-1})	96.92	33.00
	E (KJ mol^{-1})	0.181	0.475
	R^2	0.910	0.852
Temkin	A_T (L g^{-1})	0.174	0.942
	b_T	33.78	218.0
	B_T (J mol^{-1})	73.35	11.37
	R^2	0.925	0.956

The value of adsorption free energy (E) can indicate the kind of adsorption and its value can be calculated from Eq. (15):

$$E = \frac{1}{\sqrt{2B}} \tag{15}$$

If the amount of E from 8–16 kJ mol^{-1} then the process is a chemical ion exchange and if the amount of E fewer than 8 kJ mol^{-1} then it is physical adsorption. As demonstrated in Table 5 the magnitude of E was found to be lower than 8 k J mol^{-1} which indicates a physical adsorption process in both Al and Fe.

5.4. Temkin isotherm

Temkin and Pyzhev [46] suggested that the heat of adsorption of all molecules in the layer decrease with coverage due to adsorbent-adsorbate interaction. This adsorption is distinguished by an identical distribution of binding energies. The linearized form of this model is illustrated in Table 4.

A and B can be estimated from the intercept and the slope of the linear plot of data q_e vs. lnC_e. Contrary to Langmuir and Freundlich models, Temkin isotherm reflects adsorbate-adsorbent interactions. The Temkin parameters are represented in Table 5. R^2 of the Temkin isotherm model equals 0.925 and 0.956, respectively for Al and Fe.

From the data represented in Table 5, it is clear that Freundlich is the most suitable model for Al while Temkin and Langmuir are more suitable models for Fe.

6. EC kinetics studies

The mechanism of adsorption was investigated using pseudo-first-order and pseudo-second-order models [31]. The pseudo-first-order kinetic model was applied using Eq. (16):

$$\log\left(q_e - q_t\right) = \log\left(q_e\right) - \frac{k_1}{2.303}t \tag{16}$$

where q_e and q_t is the quantity of dye adsorbed on the flocs at equilibrium and at time t respectively and k_1 (min^{-1}) denotes the constant rate of the first order adsorption. The plot of log ($q_e - q_t$) vs. t provides a slope equivalent to (k_1/2.303) a straight line is obtained with correlation coefficient value R^2 close to unity (Table 6), which suggests that the adsorption of AG 20 can be elucidated by the pseudo-first-order kinetic model for both metal Al and Fe.

The pseudo-second-order kinetic model used:

$$\frac{t}{q_t} = \frac{1}{k_2 q_e^2} + \frac{t}{q_e} \tag{17}$$

where k_2 (g mg^{-1} min^{-1}) stands for the constant rate of the pseudo-second-order kinetic model. The value of k_2 can be obtained from the intercept of the plot of t/q_t vs. t (min). Table 6 illustrates the values of k_1 and k_2 of the two models. The pseudo-second-order kinetic model showed inadequate fitting for the gained results and the estimated equilibrium adsorption capacities.

Table 7 summarizes the results obtained in the comparison between Fe and Al EC processes. From the table, it can be concluded that the Fe electrode is more favored than the Al electrode for the removal of AG 20 which gave higher percent removal with lower energy consumption.

7. Removal of AG 20 by a hybrid electrode combination

The choice of electrode material is a significant parameter in EC, taking into consideration: the time of electrolysis, the % Re and the energy consumption. The removal of AG

Table 6
Parameters of the kinetic models used

Kinetic model	Kinetic parameters and regression coefficients	Aluminum	Iron
Pseudo-first-order	k_1 (min^{-1})	0.054	0.052
	R^2	**0.978**	**0.971**
Pseudo-second-order	k_2 (g mg^{-1} min^{-1})	–0.004	–0.007
	R^2	0.953	0.951

Table 7
Comparison between Al and Fe considering the most important parameters of the EC process

Parameters	Aluminum	Iron
Optimum concentration (mg L^{-1})	60	60
pH	2.0	2.0
% Re	94.81%	96.38%
Energy consumption (kWh kg^{-1} of dye)	31.02	28.84
$\Delta G°$ (kJ mol^{-1}) at 303 K	–2.832	–3.686
$\Delta H°$ (kJ mol^{-1})	–24.053	–15.215
$\Delta S°$ (J mol^{-1} K^{-1})	90.473	62.653
Kinetic model	Pseudo-first-order	Pseudo-first-order
Adsorption model	Freundlich	Temkin and Langmuir

20 was performed using Fe, Al and different combinations of them as represented in Table 8 and the connection was as represented in Fig. 2b. Iron and aluminum plate electrodes in six different hybrid combinations (anode–cathode) were used to estimate the perfect electrode pairs for the maximum removal efficiency of AG 20 dye from water.

It was found that the % Re was higher for Fe–Fe–Fe–Fe electrode pairs where the removal efficiency was 87%. The lower removal efficiency attained with the Al–Al–Al–Al electrode pairs where the removal efficiency was only 69% as shown in Fig. 16. This may be attributed to the greater solubility of the Fe electrode rather than the Al and also it may be owing to the higher adsorption capacity for the iron coagulants rather than the Aluminium one [38]. Furthermore, the iron electrodes have higher oxidation potential (–0.447 V) than the aluminum electrodes (–1.662 V). Also, the Fe electrodes provide better bubble production rather than the Al electrodes [35]. It is observed that, when the Fe electrodes were incorporated in the electrolysis with the Al, the removal efficiencies have been increased as indicated in Table 8. The hybrid electrode pairs Al–Fe–Al–Fe gave 82% removal efficiency, Fe–Al–Al–Fe electrode pairs gave 80% removal efficiency, Al–Fe–Fe–Al electrode pairs gave 79% removal efficiency and Fe–Al–Fe–Al electrode pairs gave 73% removal efficiency. All hybrid electrode pairs were able to remove the AG 20 dye up to over 70%. This result can be clarified by the reactions occurring at the Al and Fe anodes. Production of metallic cations at the anode side, and H_2 production and the release of OH^- at the cathode side (Eqs. (4–7)). The release of ferric or aluminum ions by electrochemical oxidation of Al and Fe electrodes may form monomeric species and polymeric hydroxyl metallic complexes. These complexes may provide efficient coagulation of ions and particles [47].

8. Correlation matrix and multiple regression analyses

IBM SPSS STATISTICA 22 was used to assign the correlation matrix as well as the multiple regression analyses for different variables including the mass of Fe and Al coagulants, pH, contact time, % Re, initial (C_0), and interval concentrations (C_t). Using Fe electrodes leads to the fact that the dependence of C_t on the mass of Fe coagulant (r = –0.5698; p = 0.000), and the contact time (r = –0.570; p = 0.000) is confirmed by the high correlation coefficients of correlation matrix.

Furthermore, the removal of AG 20 is highly affected by the pH value (r = 0.551; p = 0.000), contact time (r = 0.913;

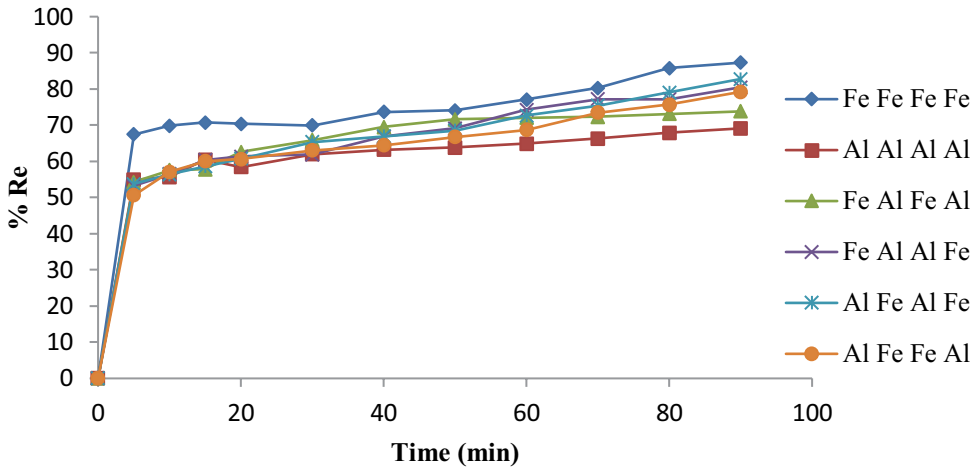

Fig. 16. Effect of different electrode combination on the removal efficiency of AG 20 at different time intervals (CD = 40 mA cm^{-2}; NaCl = 0.5 g L^{-1}; C_0 = 60 mg L^{-1}; pH_i = 2; t_{EC} = 90 min; stirring speed = 771.4 rpm; nine electrode sheets; RT).

Table 8
The effect of electrode material and combination in the presence of two sacrificial electrodes on the removal efficiency of AG 20 dye, t_{EC} = 90 min

No.	Electrode material	% Re
1	Sacrificial electrodes: Fe (anode: Fe, cathode: Fe)	87%
2	Sacrificial electrodes: Fe, Al (anode: Al, cathode: Fe)	82%
3	Sacrificial electrodes: Al (anode: Fe, cathode: Fe)	80%
4	Sacrificial electrodes: Fe (anode: Al, cathode: Al)	79%
5	Sacrificial electrodes: Al, Fe (anode: Fe, cathode: Al)	73%
6	Sacrificial electrodes: Al (anode: Al, cathode: Al)	69%

Table 9
The correlation matrix of the variables of the removal of AG 20 by EC technique

Variables	Time	Initial concentration (C_0)	Concentration at time (C_t)	% Re	Mass of Fe coagulant	pH
Time	r = 1.000					
	p = 0.000					
Initial concentration (C_0)	r = 0.000	r = 1.000				
	p = 1.000	p = 0.000				
Concentration at time (C_t)	**r = –0.570**	**r = 0.723**	r = 1.000			
	p = 0.000	p = 0.000	p = 0.000			
% Re	**r = 0.913**	r = –0.066	**r = –0.646**	r = 1.000		
	p = 0.000	p = 0.521	p = 0.000	p = 0.000		
Mass of Fe coagulant	r = 1.000	r = 0.000	**r = –0.5698**	**r = 0.913**	r = 1.000	
	p = 0.000	p = 1.000	p = 0.000	p = 0.000	p = 0.000	
pH	r = 0.340	r = –0.089	r = –0.407	**r = 0.551**	**r = 0.341**	r = 1.000
	p = 0.001	p = 0.389	p = 0.000	p = 0.000	p = 0.001	p = 0.000

The significant correlations are represented in bold.

p = 0.000) and interval times (r = –0.646; p = 0.000). Additionally, as can be seen from Table 9, the pH value (r = 0.341, p = 0.001) has affected the mass of Fe coagulant.

The following highly significant equation (Eq. (18)) that represents the AG 20 removal by EC has been given by the multiple regressions of the previously mentioned variables:

$$\text{Re}\,\% = -117.127 - 0.176C_0 - 0.309C_t + 0.664\ \text{Mass of Fe coagulant} + 0.214\ \text{pH}\ \left(R = 0.955,\ P < 0.000\right) \quad (18)$$

On the other hand, in case of using Al electrodes, the dependence of C_t on the contact time (r = –0.0.446; p = 0.000) is confirmed by the high correlation coefficients of correlation matrix. Also, the removal of AG 20 is affected by contact time (r = 0. 694; p = 0.000) and interval times (r = –0.701; p = 0.000).

Furthermore, as can be noted from Table 10, the mass of Al coagulant (r = 0.694, p = 0.000) has affected the removal of AG 20. The following highly significant equation (Eq. (19)) that represents the AG 20 removal by EC has been given by the multiple regressions of the aforementioned variables:

$$\text{Re}\,\% = 53.208 + 0.278\ \text{Time} + 0.516\ C_0 - 0.931\ C_t + 0.015\ \text{pH}\ \left(R = 0.887,\ P < 0.000\right) \quad (19)$$

9. Operating cost

Operation cost is a very important economical parameter in the EC process like all other electrolytic processes. The operating cost includes a material cost (mainly electrodes), utility cost (mainly electrical energy), hand labor and chemical product. In the present study, only specific energy consumption (E) (Eq. (11)) and electrical cost of the electrode (EIC) (Eq. (20)) are taken into account as major costs.

$$\text{EIC} = \frac{I \times \text{Mw} \times t}{n \times F \times V} \quad (20)$$

$$\text{TOC} = £\text{E} + ß\text{EIC} \quad (21)$$

where F is the Faraday constant, n represents the number of transferred electrons and Mw is the molecular mass.

For the Egyptian market (in the present study), in June 2019 the prices of electrical energy for industrial sector £ were 0.05 US$/1 KWh and for aluminum and iron electrodes ß were (0.55 and 0.5 US$/1 m^3 respectively). The results showed that total operating cost (TOC) (US$/$m^3$) for real effluent for dye using Al electrodes was (1.5 US$/$m^3$).

Table 10
The correlation matrix of the variables of the removal of AG 20 by EC technique

Variables	Time	Initial concentration (C_0)	Concentration at time (C_t)	% Re	Mass of Al coagulant	pH
Time	r = 1.000					
	p = 0.000					
Initial concentration (C_0)	r = 0.000	r = 1.000				
	p = 1.00	p = 0.000				
Concentration at time (C_t)	**r = –0.446**	**r = 0.680**	r = 1.000			
	p = 0.000	p = 0.000	p = 0.000			
% Re	**r = 0.694**	r = –0.114	**r = –0.701**	r = 1.000		
	p = 0.000	p = 0.303	p = 0.000	p = 0.000		
Mass of Al coagulant	r = 1.000	r = 0.000	**r = –0.446**	**r = 0.694**	r = 1.000	
	p = 0.000	p = 1.000	p = 0.000	p = 0.000	p = 0.000	
pH	r = 0.012	r = 0.250	r = 0.207	r = –0.046	r = 0.012	r = 1.000
	p = 0.913	p = 0.022	p = 0.059	p = 0.681	p = 0.913	p = 0.000

The significant correlations are represented in bold.

In previous work, the TOC for the removal of C.I. Basic Yellow 28 using Al electrodes was 0.07 US$ for each kg dye removed, meanwhile, the operating cost for Reactive Red 198 removal was 0.256 US$/m^3 [48].

On the other hand, in the present study, the calculated operating cost for AG 20 using Fe electrodes was (1.45 US$/m^3). For the Tunisia market, in 2018 the TOC for real indigo (1.013 US$/m^3) [49,50].

Also, the removal of Levafix Brilliant Blue E-B by the EC technique using the Al electrode has cost about 1.501 $/m^3 and about 1.526 $/m^3 for Fe electrode in the Turkish market in 2011 [51].

10. Comparison of optimized results with previous studies

Table 11 includes a comparison between the results of the present work and the results found in the previous work of different dyes (especially the acid dyes) with different reactors' configurations and different connections of different types of electrodes and other conditions. Examining the table shows that the percent removal achieved in the present work is within the accepted levels.

11. Conclusion

In the present study, the EC technique was found to be highly effective for the color removal of AG 20 dye from water. The optimum conditions were pH 2, initial concentration 60 mg L^{-1}, current density 40 mA cm^{-2}, 0.5 g L^{-1} of NaCl was effective as supporting electrolyte and the energy consumption was 28.84 and 31.02 (KWh Kg^{-1} of the dye) for Al and Fe, respectively. The computed energy consumption and total operating cost (1.5 and 1.45 US$/m^3 for Al and Fe electrodes, respectively) confirmed the economic dye removal by the EC technique. The optimum speed of stirring was 771.42 rpm and the inter-electrode gap distance was found to be 5 cm and 3.5 cm for Al and Fe, respectively. The equilibrium of the operating time was established with 20 and 30 min for Al and Fe electrodes, respectively. The effectiveness of temperature for removal of AG 20 dye was 318 and 308 K for Al and Fe, respectively. The evaluated standard thermodynamic parameters evidenced that the process is exothermic and spontaneous. Freundlich isotherm model fitted for Al while Temkin was best fitted for Fe and the adsorption procedure followed the pseudo-first-order kinetic pattern. Also, no new absorption bands emerged in the decay profile of spectra on the AG 20 solution in either the visible or ultraviolet areas which clarifies that no intermediates were formed through the EC procedure for both Al and Fe. The influence of the electrode combination showed that Fe–Fe–Fe–Fe > hybrid > Al–Al–Al–Al. Finally, the correlation matrix and multiple regression analyses were studied and predictive equations were derived.

Symbols

λ_{max} — Maximum wavelength, nm
A — Absorbance
C_0 — Initial dye concentration, mg L^{-1}
C_t — Concentration of dye at time t, mg L^{-1}
q_e — Quantity of adsorbed dye at equilibrium, mg g^{-1}
W — Mass of the metal coagulant
M — Molar mass, g mol^{-1}
I — Current, A
n — Number of electrons
F — Faraday's constant
V — Applied voltage, volt
v — Volume of solution, L
$\Delta G°$ — Standard Gibbs free energy change, kJ mol^{-1}
$\Delta S°$ — Standard entropy change, J mol^{-1} K^{-1}
$\Delta H°$ — Standard enthalpy change, kJ mol^{-1}
q_m — Saturation capacity, mg g^{-1}
K_a — Langmuir equilibrium constant, L mg^{-1}
C_e — Equilibrium concentration of adsorbate, mg L^{-1}
R_L — Separation parameter
K_f — Freundlich constant, mg g^{-1}
n_f — Constant that indicates the intensity of the adsorption

Table 11
Comparison of optimized results with previous studies

Dye	Anode	Solution pH and electrolyte	Type of system	Treatment time (min)	Current density (mA cm^{-2})	Percent removal	Reference
Acid Black 1	Fe	6.8	Stirred tank reactor with two monopolar plate electrodes in batch	12	10.7	81	[6]
Reactive Blue 4		3.8				84	
Acid Red 87		5.8 with 0.1 g dm^{-3} NaCl				39	
Acid Blue 113	Fe	6.5 with 2.0 g dm^{-3}	Tank reactor with two monopolar plate electrodes in batch without stirring	60	30	95	[52]
Reactive Black 5	Fe	6.6 with 2 g dm^{-3} NaCl or Na_2SO_4	Stirred tank reactor with two monopolar plate electrodes in batch	20	7.5	82 with Na_2SO_4 93 with NaCl	[53]
Acid Black 52	Al	5 with 2 g dm^{-3}	Stirred tank reactor with two monopolar plate electrodes in batch	7.5	4	90	[27]
Acid Yellow 220						98	
Acid Black 172	Al	7 with NaCl	Stirred tank reactor with four monopolar plate electrodes in batch	9.1	8.3	90	[54]
Basic Green 4	Al	6.2 with 1.5 g dm^{-3}	Tank reactor with two monopolar plate electrodes in batch without stirring	45	11.7	99	[55]
Acid Blue 19	Fe	6.1 with Na_2SO_4	Stirred tank reactor with two monopolar plate electrodes in batch	4	10	95	[56]
	Al					29	
Basic Violet 3	Fe	5.8 with 284 mg dm^{-3} Na_2SO_4	Stirred tank reactor with three monopolar anodes and four monopolar cathodes in batch	5	2.8	95	[57]
	Al					90	
Reactive Red 43	Fe	6.5 with 0.04 N NaCl	Stirred tank reactor with two monopolar anodes and two monopolar cathodes in batch	24	2.5	99	[58]
	Al					77	
Acid Green 50	Al	6.9 with 1 g L^{-1} NaCl	Cylindrical reactor. Anode is a cylindrical aluminum sheet lining the inner wall and the bottom of the vessel, cathode is a cylindrical aluminum screen cathode having geometry similar to the anode was placed at a distance of 1 cm from the anode.	21	1.67	98	[59]
Acid Green 20	Al	2.1 with 0.5 g L^{-1} NaCl	A batch stirred reactor with 9 electrodes in bipolar series connection	90	40	94.81	Present work
	Fe					96.38	

B — Constant related to the free energy of adsorption, mol^2 kJ^{-2}
ε — Polanyi potential
R — Ideal gas constant, J mol^{-1} K^{-1}
E — Free energy of adsorption, kJ mol^{-1}
B_T — Temkin constant related to the heat of adsorption
b_T — Temkin isotherm constant, J mol^{-1}
A_T — Temkin constant corresponding to the maximum binding energy, L g^{-1}
k_1 — First-order rate constant, min^{-1}
k_2 — Pseudo-second-order rate constant, g mg^{-1} min^{-1}
q_t — Quantity of adsorbed dye at time t
£ — Prices of electrical energy for the industrial sector
β — Prices of electrodes
US$ — United States Dollar
TOC — Total operating cost

References

[1] A.K. Verma, Treatment of textile wastewaters by electrocoagulation employing Fe-Al composite electrode, J. Water Process Eng., 20 (2017) 168–172.
[2] J.-S. Bae, H.S. Freeman, Aquatic toxicity evaluation of new direct dyes to the *Daphnia magna*, Dyes Pigm., 73 (2007) 81–85.
[3] D.P. Chattopadhyay, Chapter 4 – Chemistry of Dyeing, M. Clark, Ed., Handbook of Textile and Industrial Dyeing: Principles, Processes and Types of Dyes, Woodhead Publishing, UK, 2011, pp. 150–183.
[4] S. Zodi, B. Merzouk, O. Potier, F. Lapicque, J.-P. Leclerc, Direct red 81 dye removal by a continuous flow electrocoagulation/flotation reactor, Sep. Purif. Technol., 108 (2013) 215–222.
[5] M. Yousuf A. Mollah, R. Schennach, J.R. Parga, D.L. Cocke, Electrocoagulation (EC) — science and applications, J. Hazard. Mater., B84 (2001) 29–41.
[6] M.-C. Wei, K.-S. Wang, C.-L. Huang, C.-W. Chiang, T.-J. Chang, S.-S. Lee, S.-H. Chang, Improvement of textile dye removal by electrocoagulation with low-cost steel wool cathode reactor, Chem. Eng. J., 192 (2012) 37–44.
[7] A.E. Yilmaz, R. Boncukcuoğlu, M. Kocakerim, İ.H. Karakaş, Waste utilization: the removal of textile dye (Bomaplex Red CR-L) from aqueous solution on sludge waste from electrocoagulation as adsorbent, Desalination, 277 (2011) 156–163.
[8] A. Pirkarami, M.E. Olya, Removal of dye from industrial wastewater with an emphasis on improving economic efficiency and degradation mechanism, J. Saudi Chem. Soc., 21 (2017) S179–S186.
[9] U. Tezcan Un, A.S. Koparal, U. Bakir Ogutveren, Electrocoagulation of vegetable oil refinery wastewater using aluminum electrodes, J. Environ. Manage., 90 (2009) 428–433.
[10] E. Bazrafshan, L. Mohammadi, A. Ansari-Moghaddam, A.H. Mahvi, Heavy metals removal from aqueous environments by electrocoagulation process – a systematic review, J. Environ. Health Sci. Eng., 13 (2015) 74.
[11] M. Al-Shannag, Z. Al-Qodah, K. Bani-Melhem, M.R. Qtaishat, M. Alkasrawi, Heavy metal ions removal from metal plating wastewater using electrocoagulation: kinetic study and process performance, Chem. Eng. J., 260 (2015) 749–756.
[12] D. Ghosh, H. Solanki, M.K. Purkait, Removal of Fe(II) from tap water by electrocoagulation technique, J. Hazard. Mater., 155 (2008) 135–143.
[13] R. Kamaraj, P. Ganesan, S. Vasudevan, Removal of lead from aqueous solutions by electrocoagulation: isotherm, kinetics and thermodynamic studies, Int. J. Environ. Sci. Technol., 12 (2013) 683–692.
[14] A.A. Moneer, A.A. El-Shafei, M.M. Elewa, M.M. Naim, Removal of copper from simulated wastewater by electrocoagulation/floatation technique, Desal. Water Treat., 57 (2015) 22824–22834.
[15] J.R. Parga, D.L. Cocke, J.L. Valenzuela, J.A. Gomes, M. Kesmez, G. Irwin, H. Moreno, M. Weir, Arsenic removal via electrocoagulation from heavy metal contaminated groundwater in La Comarca Lagunera Mexico, J. Hazard. Mater., 124 (2005) 247–254.
[16] A. Shafaei, E. Pajootan, M. Nikazar, M. Arami, Removal of Co(II) from aqueous solution by electrocoagulation process using aluminum electrodes, Desalination, 279 (2011) 121–126.
[17] U.T. Un, S.E. Ocal, Removal of heavy metals (Cd, Cu, Ni) by electrocoagulation, Int. J. Environ. Sci. Dev., 6 (2015) 425–429.
[18] W. Perren, A. Wojtasik, Q. Cai, Removal of microbeads from wastewater using electrocoagulation, ACS Omega, 3 (2018) 3357–3364.
[19] X.M. Chen, G.H. Chen, P.L. Yue, Separation of pollutants from restaurant wastewater by electrocoagulation, Sep. Purif. Technol., 19 (2000) 65–76.
[20] N. Drouiche, N. Ghaffour, H. Lounici, M. Mameri, Electrocoagulation of chemical mechanical polishing wastewater, Desalination, 214 (2007) 31–37.
[21] C.L. Lai, S.H. Lin, Electrocoagulation of chemical mechanical polishing (CMP) wastewater from semiconductor fabrication, Chem. Eng. J., 95 (2003) 205–211.
[22] S. Garcia-Segura, M.M.S.G. Eiband, J.V. de Melo, C.A. Martínez-Huitle, Electrocoagulation and advanced electrocoagulation processes: a general review about the fundamentals, emerging applications and its association with other technologies, J. Electroanal. Chem., 801 (2017) 267–299.
[23] C. Barrera-Díaz, F. Ureña-Nuñez, E. Campos, M. Palomar-Pardavé, M. Romero-Romo, A combined electrochemical-irradiation treatment of highly colored and polluted industrial wastewater, Radiat. Phys. Chem., 67 (2003) 657–663.
[24] G. Mouedhen, M. Feki, M. de Petris Wery, H.F. Ayedi, Behavior of aluminum electrodes in electrocoagulation process, J. Hazard. Mater., 150 (2008) 124–135.
[25] A.S. Fajardo, R.C. Martins, D.R. Silva, C.A. Martínez-Huitle, R.M. Quinta-Ferreira, Dye wastewaters treatment using batch and recirculation flow electrocoagulation systems, J. Electroanal. Chem., 801 (2017) 30–37.
[26] M.S. Mahmoud, J.Y. Farah, T.E. Farrag, Enhanced removal of Methylene Blue by electrocoagulation using iron electrodes, Egypt. J. Pet., 22 (2013) 211–216.
[27] E. Pajootan, M. Arami, N.M. Mahmoodi, Binary system dye removal by electrocoagulation from synthetic and real colored wastewaters, J. Taiwan Inst. Chem. Eng., 43 (2012) 282–290.
[28] J.N. Hakizimana, B. Gourich, M. Chafi, Y. Stiriba, C. Vial, P. Drogui, J. Naja, Electrocoagulation process in water treatment: a review of electrocoagulation modeling approaches, Desalination, 404 (2017) 1–21.
[29] E. Brillas, C.A. Martínez-Huitle, Decontamination of wastewaters containing synthetic organic dyes by electrochemical methods. An updated review, Appl. Catal., B, 166–167 (2015) 603–643.
[30] C.J. Izquierdo, P. Canizares, M.A. Rodrigo, J.P. Leclerc, G. Valentin, F. Lapicque, Effect of the nature of the supporting electrolyte on the treatment of soluble oils by electrocoagulation, Desalination, 255 (2010) 15–20.
[31] A.A. Moneer, M.M. El-Sadaawy, G.F. El-Said, F.A.M. Morsy, Modeling adsorption kinetic of crystal violet removal by electrocoagulation technique using bipolar iron electrodes, Water Sci. Technol., 77 (2018) 323–336.
[32] C.-H. Huang, L. Chen, C.-L. Yang, Effect of anions on electrochemical coagulation for cadmium removal, Sep. Purif. Technol., 65 (2009) 137–146.
[33] M.M. Naim, A.A. Moneer, G.F. El-Said, Predictive equations for the defluoridation by electrocoagulation technique using bipolar aluminum electrodes in the absence and presence of additives: a multivariate study, Desal. Water Treat., 57 (2015) 6320–6332.
[34] V. Khandegar, A.K. Saroha, Electrocoagulation for the treatment of textile industry effluent – a review, J. Environ. Manage., 128 (2013) 949–963.
[35] S. Barışçı, O. Turkay, Domestic greywater treatment by electrocoagulation using hybrid electrode combinations, J. Water Process Eng., 10 (2016) 56–66.

[36] B.N. Patil, D.B. Naik, V.S. Shrivastava, Photocatalytic degradation of hazardous Ponceau-S dye from industrial wastewater using nanosized niobium pentoxide with carbon, Desalination, 269 (2011) 276–283.
[37] F.I. El-Hosiny, K.A. Selim, M.A. Abdel-Khalek, I. Osama, Physicochemical study of dye removal using electro-coagulation-flotation process, Physicochem. Probl. Miner. Process., 54 (2018) 321–333.
[38] N. Modirshahla, M.A. Behnajady, S. Mohammadi-Aghdam, Investigation of the effect of different electrodes and their connections on the removal efficiency of 4-nitrophenol from aqueous solution by electrocoagulation, J. Hazard. Mater., 154 (2008) 778–786.
[39] I. Langmuir, The adsorption of gases on plane surfaces of glass, mica and platinum, J. Am. Chem. Soc., 40 (1918) 1361–1403.
[40] J. Kiurski, S. Adamovic, J. Krstic, I. Oros, M.V. Miloradov, Adsorption efficiency of low-cost materials in the removal of Zn(II) ions from printing developer, Acta Tech. Corviniensis – Bull. Eng., 4 (2011) 61.
[41] A. Hussain, A. Ghafoor, M. Anwar-Ul-Haq, M. Nawaz, Application of the Langmuir and Freundlich equations for P adsorption phenomenon in saline-sodic soils, Int. J. Agric. Biol., 5 (2003) 1560–8530.
[42] F. Gao, Y.W. Xue, P.Y. Deng, X.R. Cheng, K. Yang, Removal of aqueous ammonium by biochars derived from agricultural residuals at different pyrolysis temperatures, Chem. Speciation Bioavailability, 27 (2015) 92–97.
[43] H. Freundlich, Über die adsorption in lösungen, Zeitschrift für physikalische Chemie, 57 (1907) 385–470.
[44] A.O. Dada, A.P. Olalekan, A.M. Olatunya, O. Dada, Langmuir, Freundlich, Temkin and Dubinin–Radushkevich isotherms studies of equilibrium sorption of Zn^{2+} unto phosphoric acid modified rice husk, IOSR J. Appl. Chem., 3 (2012) 38–45.
[45] A. Günay, E. Arslankaya, I. Tosun, Lead removal from aqueous solution by natural and pretreated clinoptilolite: adsorption equilibrium and kinetics, J. Hazard. Mater., 146 (2007) 362–371.
[46] M.J. Temkin, V. Pyzhev, Kinetics of ammonia synthesis on promoted iron catalysts, Acta Physicochim. URSS, 12 (1940) 217–222.
[47] M. Kobya, A. Akyol, E. Demirbas, M.S. Oncel, Removal of arsenic from drinking water by batch and continuous electrocoagulation processes using hybrid Al-Fe plate electrodes, Environ. Prog. Sustainable Energy, 33 (2014) 131–140.
[48] A. Dalvand, M. Gholami, A. Joneidi, N.M. Mahmoodi, Dye removal, energy consumption and operating cost of electrocoagulation of textile wastewater as a clean process, CLEAN – Soil Air Water, 39 (2011) 665–672.
[49] K. Hendaoui, F. Ayari, I.B. Rayana, R.B. Amar, F. Darragi, M. Trabelsi-Ayadi, Real indigo dyeing effluent decontamination using continuous electrocoagulation cell: study and optimization using response surface methodology, Process Saf. Environ. Prot., 116 (2018) 578–589.
[50] N. Daneshvar, A.R. Khataee, N. Djafarzadeh, The use of artificial neural networks (ANN) for modeling of decolorization of textile dye solution containing C.I. Basic Yellow 28 by electrocoagulation process, J. Hazard. Mater., 137 (2006) 1788–1795.
[51] F. Akbal, A. Kuleyin, Decolorization of levafix brilliant blue E-B by electrocoagulation method, Environ. Prog. Sustainable Energy, 30 (2011) 29–36.
[52] M. Saravanan, N.P. Sambhamurthy, M. Sivarajan, Treatment of Acid Blue 113 dye solution using iron electrocoagulation, CLEAN – Soil Air Water, 38 (2010) 565–571.
[53] U.D. Patel, J.P. Ruparelia, M.U. Patel, Electrocoagulation treatment of simulated floor-wash containing Reactive Black 5 using iron sacrificial anode, J. Hazard. Mater., 197 (2011) 128–136.
[54] M. Taheri, M.R.A. Moghaddam, M. Arami, Optimization of Acid Black 172 decolorization by electrocoagulation using response surface methodology, Iran. J. Environ. Health Sci. Eng., 9 (2012) 23.
[55] S. Singh, V.C. Srivastava, I.D. Mall, Mechanistic study of electrochemical treatment of Basic Green 4 dye with aluminum electrodes through zeta potential, TOC, COD and color measurements, and characterization of residues, RSC Adv., 3 (2013) 16426–16439.
[56] A. Olad, A.R. Amani-Ghadim, M.S.S. Dorraji, M.H. Rasoulifard, Removal of the alphazurine FG dye from simulated solution by electrocoagulation, CLEAN–Soil Air Water, 38 (2010) 401–408.
[57] P. Durango-Usuga, F. Guzmán-Duque, R. Mosteo, M.V. Vazquez, G. Peñuela, R.A. Torres-Palma, Experimental design approach applied to the elimination of crystal violet in water by electrocoagulation with Fe or Al electrodes, J. Hazard. Mater., 179 (2010) 120–126.
[58] A.R. Amani-Ghadim, A. Olad, S. Aber, H. Ashassi-Sorkhabi, Comparison of organic dyes removal mechanism in electrocoagulation process using iron and aluminum anodes, Environ. Prog. Sustainable Energy, 32 (2013) 547–556.
[59] E.-S.Z. El-Ashtoukhy, N.K. Amin, Removal of acid green dye 50 from wastewater by anodic oxidation and electrocoagulation—a comparative study, J. Hazard. Mater., 179 (2010) 113–119.